Measurements of electron density and temperature in the H-1 heliac plasma by helium line intensity ratios

Shuiliang Ma,[a] John Howard, Boyd D. Blackwell, and Nandika Thapar
Plasma Research Laboratory, Australian National University, Canberra ACT 0200, Australia

(Received 18 October 2011; accepted 19 February 2012; published online 7 March 2012)

Electron density and temperature distributions in the H-1 heliac plasma are measured using the helium line intensity ratio technique based on a collisional–radiative model. An inversion approach with minimum Fisher regularization is developed to reconstruct the ratios of the local emission radiances from detected line-integrated intensities. The electron density and temperature inferred from the He I 667.8/728.1 and He I 728.1/706.5 nm line ratios are in good agreement with those from other diagnostic techniques in the inner region of the plasma. The electron density and temperature values appear to be a little high in the outer region of the plasma. Some possible causes of the discrepancy in the outer region are discussed. © *2012 American Institute of Physics*. [http://dx.doi.org/10.1063/1.3692756]

I. INTRODUCTION

Knowledge of electron density (n_e) and temperature (T_e) at the edge of fusion plasmas is essential for understanding physical issues such as radiation loss, impurity fluxes, and particle and power transport. Methods for measuring plasma n_e and T_e include interferometry, spectroscopy, electron cyclotron emission (ECE), Thomson scattering, probes, and so on.[1] For the H-1 heliac device,[2] many diagnostic methods have been deployed for the determination of the plasma parameters.[3–8] However, there are limitations which preclude the use of some standard electron temperature diagnostic methods. For example, the H-1 plasma is not optically thick enough for ECE, and n_e is too low for Thomson scattering. The limitation of probes is that they will possibly perturb the plasma and cannot be used in high temperature regions, in which they will be destroyed due to the high heat fluxes. While the n_e distributions can be measured by an interferometer.[4] For the determination of T_e distributions, only the spectroscopic methods[6–8] remain a feasible option.

Among spectroscopic methods, the helium line intensity ratio technique is a simple and fairly reliable approach for the measurement of n_e and T_e. It relies on measurement of the relative intensities of various atomic spectral lines whose ratio is a strong function of n_e or T_e. One important advantage of this technique is that only the relative intensity calibration is needed, and this makes it very easy for implementation compared with other spectroscopic methods. Due to the considerable developments in the calculation of accurate cross-section data for neutral helium during the last few decades,[9,10] the theoretical line intensity ratios calculated based on a collisional–radiative (CR) model[11,12] are becoming more reliable. This has seen the technique now commonly deployed for the measurement of n_e and T_e in the edge region of fusion plasmas and in some other plasmas.[7,8,13–25] These measurements give n_e and T_e values that are consistent with results from other diagnostic techniques, such as probes, Thomson scattering, and interferometry.[19–25]

In this work, the helium line intensity ratio technique is applied to the measurement of n_e and T_e distributions in the H-1 heliac plasma. It is planned to use the inferred plasma n_e and T_e information for characterizing the plasma temperature and density fluctuations.[26] In Sec. II, the tomography approach for reconstructing spectral line radiances and radiance ratios from line-of-sight measurements and the helium line intensity ratio technique based on a CR model are described. Section III provides the experimental details for measuring helium line intensities. In Sec. IV, we show the experimental results that are discussed in comparison with values from other diagnostic techniques. Finally, Sec. V gives the conclusions.

II. TOMOGRAPHY AND DIAGNOSTIC TECHNIQUES

A. Tomography for reconstructing spectral line ratios

Spectral line intensities from transitions of plasma species are determined by spontaneous emission, stimulated emission, and absorption in plasmas. When both stimulated emission and absorption are negligible compare to spontaneous emission, the corresponding spectral line can be considered optically thin. The optical opacity of several helium spectral lines has been analyzed in Ref. 15, and the effect of radiation trapping on the measurement of n_e and T_e by helium line intensity ratio technique has been considered in Refs. 21–23 and 27. For simplicity, we assume the plasma is optically thin for the measured spectral lines, i.e., it is fully transparent to the radiation to be measured. In this case, the plasma light intensity detected is approximated as the integration of the local plasma radiance along the line-of-sight path, which can be expressed as

$$f(p,\varphi) = \int_l g(r,\theta)dl, \tag{1}$$

where $g(r, \theta)$ is the local plasma radiance with r and θ the polar coordinates. For the observed plasma intensity $f(p, \varphi)$, the integrations over collection solid angle and local volume elements are treated as an ideal line-integral with p the perpendicular distance from the coordinate origin to the chord

[a]Electronic mail: shuiliang.ma@anu.edu.au.

line, φ the chord angle, and l represents the line-of-sight path of the measurement. We shall use the term radiance to refer to the local plasma line emission and intensity to refer to the projected (measured) quantities.

To obtain the local plasma radiance distributions, usually a large number of measurements with different perpendicular distances and chord angles are required. In a special case for fusion plasmas, it is often the case that the plasma emission can be assumed to be homogenous along magnetic field lines. In this case measurements in only one view direction are needed to obtain a reconstruction and Eq. (1) can be discretized as

$$f_i = \sum_{j=0}^{N} T_{ij} g_j, \quad \mathbf{f} = \mathbf{T} * \mathbf{g}, \tag{2}$$

where $i = 0, 1, \ldots, M$, is the number of measurements, $j = 0, 1, \ldots, N$, is the number of radial zones of the reconstruction domain being discretized, and T_{ij} is the length of intersection of the ith measurement viewing chord with the jth plasma zone (annular flux rings in magnetic coordinates). Because helium atoms are not charged, the assumption of constant emissivity on flux surfaces is not necessarily true for the atomic emissions. Nevertheless, as will be seen, the quality of the tomographic fit to the projection measurements indicates that the approximation is reasonable in the H-1 case.

Equation (2) can represent an under-determined ($M < N$) or over-determined ($M > N$) system. With the development of charge-coupled device technologies, the value of M can be ~1000, while the value of N is usually much smaller. Therefore, in most cases we solve an over-determined system, which has the advantage of insensitivity to noise. To determine the values of $\mathbf{g}$ in the over-determined system, many techniques such as least-squares fit (LSF), linear regularization (LR), maximum entropy, and minimum Fisher regularization (MFR) methods have been used (see Ref. 28, and references therein). The LR method applies a smoothing constraint on the solution and thus yields better results than the LSF method. The MFR is essentially a weighted LR method, which ensures that the low $\mathbf{g}$ regions are particularly smooth while smoothing can be decreased where $\mathbf{g}$ is large, and also has the ability to force the solution to be positive. We adopt this approach for the reconstruction of plasma radiance and local ratios.

Based on the MFR method, the solution $\mathbf{g}$ can be obtained with[28]

$$(\tilde{\mathbf{T}}^{\mathrm{T}} * \tilde{\mathbf{T}} + \alpha \mathbf{H}^{(n)}) * \mathbf{g}^{(n+1)} = \tilde{\mathbf{T}} * \tilde{\mathbf{f}}, \tag{3}$$

where $\alpha > 0$ is a regularization parameter for controlling the smoothness of the solution, $\tilde{\mathbf{T}} = \mathbf{T}/\sigma$ and $\tilde{\mathbf{f}} = \mathbf{f}/\sigma$ with σ the standard deviation of $\mathbf{f}$, and $\mathbf{H}^{(n)} = \nabla^{\mathrm{T}} * \mathbf{W}^{(n)} * \nabla$ with ∇ the finite-difference matrix,[29] $W_{ij}^{(n)} = \delta_{ij}/g_j^{(n)}$ for $g_j^{(n)} > 0$ and $W_{ij}^{(n)} = \delta_{ij}/g_{\min} > 0$ for $g_j^{(n)} \le 0$. The superscript (n) denotes the nth iteration with the initial matrix $\mathbf{W}^{(0)} \equiv 1$ and $g_{\min}$ is the value used for controlling the upper bound of the weights $W_{ij}^{(n)}$. It should be noted that, if $\mathbf{W}^{(0)} = 1$ Eq. (3) becomes the LR method, and if $\alpha = 0$ Eq. (3) becomes the LSF method.

To infer local values of n_e and T_e, it is preferable to directly reconstruct the local ratio of two spectral radiances. The smoothing constraint on the local radiance ratio of two spectral lines can also be realized using the MFR method. Based on Eq. (2) and with $r_j^{ab} = g_j^a/g_j^b$, we get

$$f_i^a = \sum_{j=0}^{N} T_{ij} g_j^a = \sum_{j=0}^{N} (T_{ij} g_j^b) r_j^{ab}, \quad \mathbf{f}^a = \mathbf{T}^b * \mathbf{r}^{ab}. \tag{4}$$

Therefore, we first reconstruct the plasma radiance profile for one spectral line $\mathbf{g}^b$, and then obtain the smooth radiance ratio profile $\mathbf{r}^{ab}$, using the MFR method similar to Eq. (3).

B. Helium line intensity ratio technique for n_e and T_e measurements

The helium line ratio technique for plasma n_e and T_e measurements is based on the fact that the intensity ratio between two singlet spectral lines is a strong function of n_e and the intensity ratio between the triplet and singlet spectral lines is a strong function of T_e, respectively. The n_e dependence is ascribed to the l-changing processes, which ensure the population ratios of the two singlet levels are close to the statistical weight ratio of these levels with increasing n_e.[19] The T_e dependence is attributed to the excitation rate coefficients from the ground state which differ significantly between the singlet levels and the triplet levels.[19]

For the determination of plasma n_e and T_e values from experimental helium line intensities, the theoretical intensity ratios are calculated based on a CR model for neutral helium developed by Fujimoto[11] and Goto.[12] Rate coefficients have been updated by Goto after the publishing of his paper (Ref. 12). The latest transition rates data by Drake (see Ref. 9) and tabulated by Wiese and Fuhr[10] have also been used. The energy levels, excepting the ground state, are assumed to satisfy the quasi-static approximation.[26] The recombining plasma component is neglected, since the ionizing plasma component is the dominant part for $n_e < 10^{14}$ cm^{-3} and $T_e > 5$ eV.[13] The ionizing plasma condition does not require the neutral density to be measured and this simplifies the diagnostic.

Figure 1(a) shows the calculated He I 667.8/728.1 nm line intensity ratios as a function of n_e for several T_e values. The intensity ratio is a strong function of n_e for $n_e > 10^{12}$ cm^{-3}, while it is almost independent of n_e for $n_e < 0.5 \times 10^{12}$ cm^{-3} (corona model[17]). This indicates that the lower n_e measurement limit for this line ratio is about 10^{12} cm^{-3}. Figure 1(b) shows the calculated He I 728.1/706.5 nm line intensity ratios as a function of T_e with several n_e values; the line intensity ratio depends on both T_e and n_e. Since these two line intensity ratios are n_e and T_e cross-dependent, to decrease the diagnostic uncertainties, it is important to perform simultaneous measurements of the three helium line intensities.

III. EXPERIMENTAL DETAILS

The experiments were conducted on the H-1 heliac stellarator with major radius $R_0 = 1.0$ m and minor radius

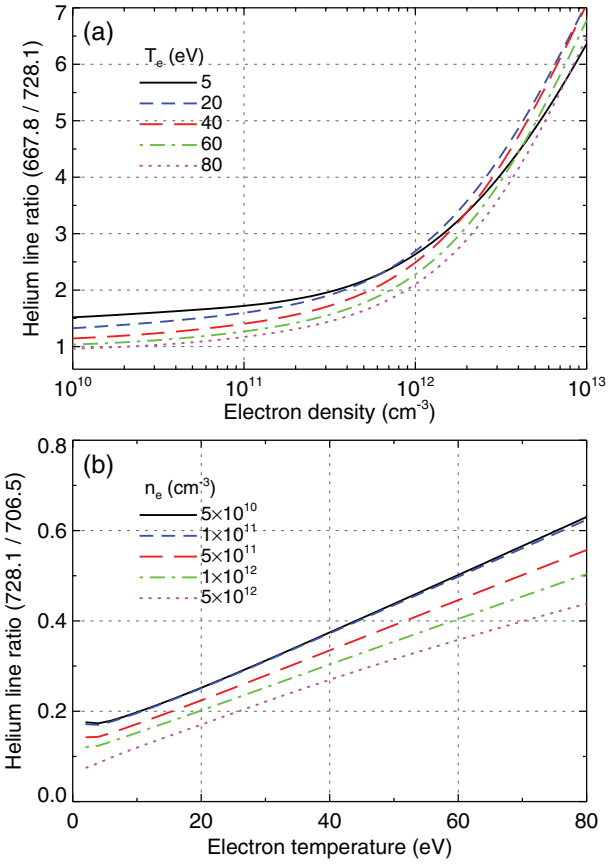

FIG. 1. Calculated line intensity ratios with several T_e and n_e values for the ionizing plasma: (a) He I 667.8/728.1 nm, for the measurement of n_e, and (b) He I 728.1/706.5 nm, for the measurement of T_e.

$a \leq 0.2$ m. The H-1 was operated at low magnetic field (0.5 T) with the current free plasma produced by the pulsed radio-frequency (RF) power of less than 100 kW at 7 MHz. The plasma in the H-1 device has typical parameters of n_e about 10^{12} cm^{-3} and T_e to be less than 20–30 eV in argon and less than 40–60 eV in helium, as studied using various diagnostics including probes, spectroscopy, and interferometry.[3–6] In this work, helium and hydrogen fill the vacuum chamber with partial pressures of 1.8×10^{-5} and 1.06×10^{-5} Torr, respectively. The plasma was formed in the magnetic configuration with control parameters $\kappa_h = I_{hw}/I_{ring} = 0.83$ (ratio of the currents in helical winding to that of the central ring conductor) and $\kappa_v = I_{ovf}/I_{ring} = 0$ (ratio of the currents in outer vertical field coils to that of central ring conductor). Figure 2 shows a typical time evolution of the line-averaged n_e horizontally across the center of the plasma poloidal cross section, measured during one discharge by a 2-mm interferometer which can be scanned vertically to tomographically determine plasma n_e distributions.

The optical setup for the measurement of helium line intensities including the viewing geometry of the camera and the collection optics is shown in Fig. 3. Light from the poloidal cross section of the plasma is collected by a first objective lens (focal length 20 mm) and then collimated by a 50 mm lens (#2 the figure) before traversing the interference filter before finally being focused at the image plane of the camera by a final 50 mm lens. The interference filters that

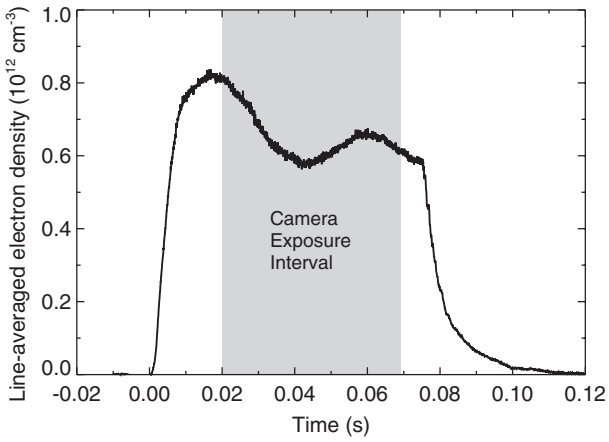

FIG. 2. Time evolution of the line-averaged n_e, measured in a discharge using the 2 mm interferometer with the vertical position close to the plasma center. Shaded area represents the camera exposure interval for the measurement of helium line intensities; the camera exposure time is about 2.7 ms, see text for more details.

were used to measure the intensities of the neutral helium lines, He I 667.8, 706.5, and 728.1 nm, have full width at half maximum about 3 nm, and effectively reject unwanted plasma emission. The PI-MAX camera from Roper Scientific is a gated and intensified camera capable of acquiring 16-bit gray images with 512 × 512 pixels corresponding to the detector sensor size of 12.4 × 12.4 mm^2. The system was originally designed for the measurement of plasma magnetohydrodynamic fluctuations, with the exposure gates synchronized to the quasi-coherent magnetic field pickup coil signal. Due to the very weak helium line intensities from the plasma, each measurement at a given phase of the plasma fluctuation was accumulated about 900 times with a gate width of 3 μs to increase the signal-to-noise ratio (the camera exposure interval is indicated by the shaded area in Fig. 2).

Since the line intensity ratio technique is used for the determination of plasma n_e and T_e values, only the relative intensity calibration is needed. The relative spatial response of the optical system was calibrated using a helium lamp before and after the experiment for measuring intensities of each of the three helium lines. The helium lamp was posed in the front

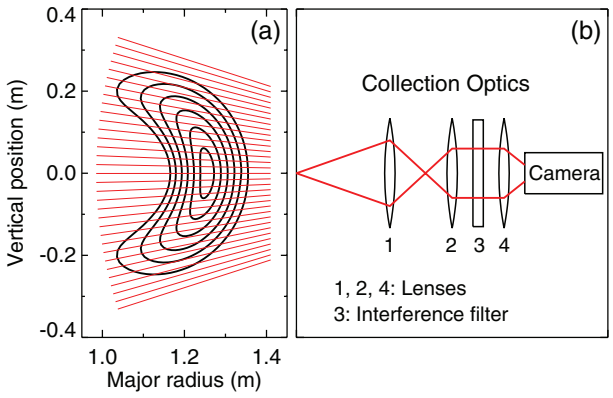

FIG. 3. Schematic of the optical system installed on the H-1 heliac plasma for measuring helium line intensities: (a) camera viewing chords geometry and (b) collection optics.

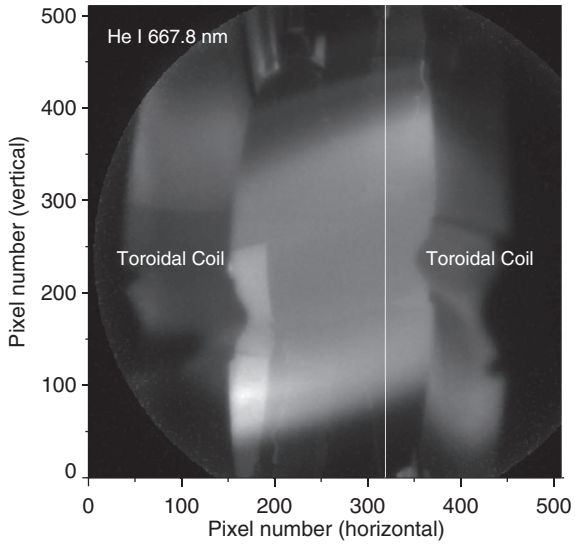

FIG. 4. An example of the measured plasma intensity images of the He I 667.8 nm line after calibration. The vertical line shows the position of the slice used for determining n_e and T_e.

of an integrative sphere to obtain the uniform light source for the calibration. The relative intensities of the helium lamp at the wavelengths of the three helium lines had been previously calibrated with a black body. The calibration source cannot be placed inside the vacuum chamber, thus the difference in the window optical efficiency at the wavelengths of the three helium lines is not included. This effect is expected to be negligible due to the close proximity of the targeted spectral lines. The uncertainty on the line intensity ratios for measuring n_e and T_e, due to uncertainties associated with the relative calibration and the light source, is estimated to be less than 10%.

IV. RESULTS AND DISCUSSION

The intensity images for the three helium lines, He I 667.8, 706.5, and 728.1 nm, were obtained by averaging over the set of phase-resolved images of the fluctuating plasma emission. Figure 4 shows a typical averaged intensity image for the He I 667.8 nm line after calibration using the uniform emission from the helium lamp and integrating sphere. Visible on the left and right sides of the image are the toroidal coils. Between these two coils is the plasma, which is brighter near the top and bottom, indicating that the emission is predominantly edge localized. Some reflections from the coils and other components in the vacuum chamber can be clearly seen from the image.

For the reconstruction of helium line radiance distributions, a vertical intensity profile was obtained from each of the calibrated spectral line images. The position of the slice, as marked in Fig. 4, is chosen to maximize the up-down symmetry of the profiles. Figure 5 shows the intensity profiles of the three helium lines measured for determining n_e and T_e. All these profiles are hollow near the plasma center. Due to the reflection from components in the vacuum chamber, and possible non-uniformity of the atom density distribution, the intensities near the center and at one edge of the intensity profiles are slightly contaminated. To reduce the effect of these reflections, the profile near the center (weak perturbation) was corrected by fitting the measured data with great attention and the profile at the right edge was replaced by the part at the left which is not affected by reflections.

After subtraction of the background "dark" image, the corrected intensity profiles were inverted assuming flux surface symmetry to obtain the radial plasma radiance distributions. The profiles for the three helium lines reconstructed with the LSF and MFR methods are presented in Fig. 6. All these profiles are hollow near the plasma center due to the plasma ionization. Since the inversion system is largely over determined ($M = 512$ and $N = 80$), the LSF method yields relatively clean results. However, a smoother reconstruction is obtained using the MFR method. The smoothing advantages with the MFR method are more apparent in noisier or less well constrained problems.

Figure 7 shows the tomographically inverted radiance ratio profiles for the determination of local n_e and T_e distributions. These profiles are obtained using three different methods, i.e., ratios derived from the separately inverted local radiance profiles (see Fig. 6) that are reconstructed with the LSF and MFR methods, respectively, and the ratio directed reconstructed using the MFR method based on Eq. (4) with

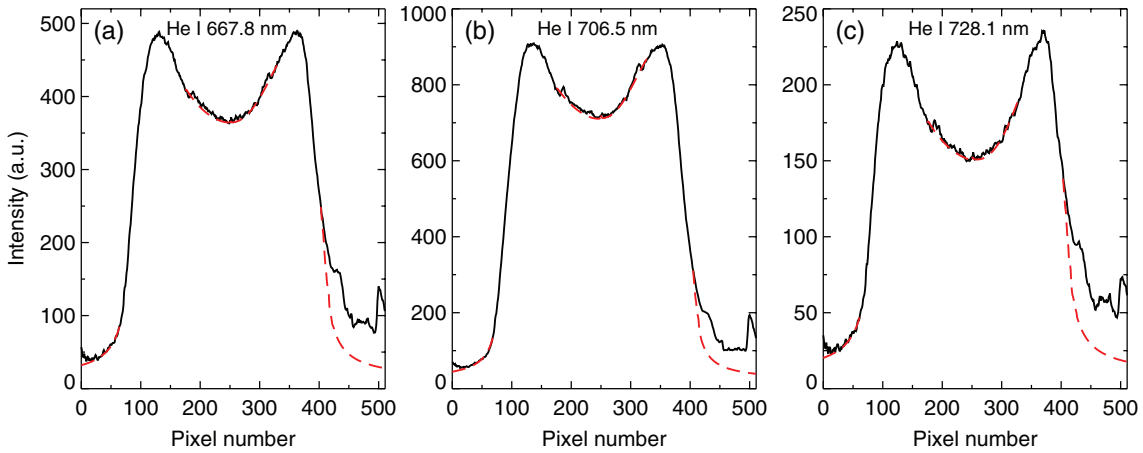

FIG. 5. Intensity profiles from one vertical slice of the intensity images for three helium lines: (a) He I 667.8 nm, (b) He I 706.7 nm, and (c) He I 728.1 nm. The dashed lines represent the profiles corrected the reflections at the center and edges of the plasma.

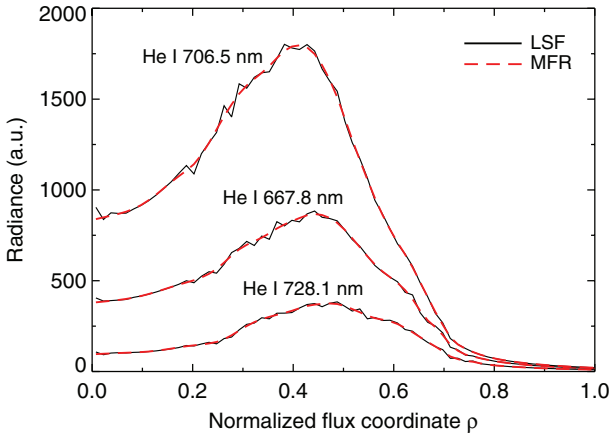

FIG. 6. Radial plasma radiance profiles for the He I 667.8, 706.7, and 728.1 nm lines reconstructed with the LSF and MFR methods.

previously inverted radiance profiles using the LSF method. The profile obtained from the ratios of the MFR inverted radiances is less noisy than the profile obtained from the ratios of the LSF inverted radiances. On the other hand, the direct inversion with the MFR method smoothes both the small and large scale fluctuations and yields a much better result. Based on these comparisons, it is clear that the direct inversion with the MFR method is most suitable for deducing the local radiance ratio profiles for inferring local n_e and T_e profiles.

Figure 7 also shows the intensity ratios directly calculated from the line-integrated intensity profiles (the left parts

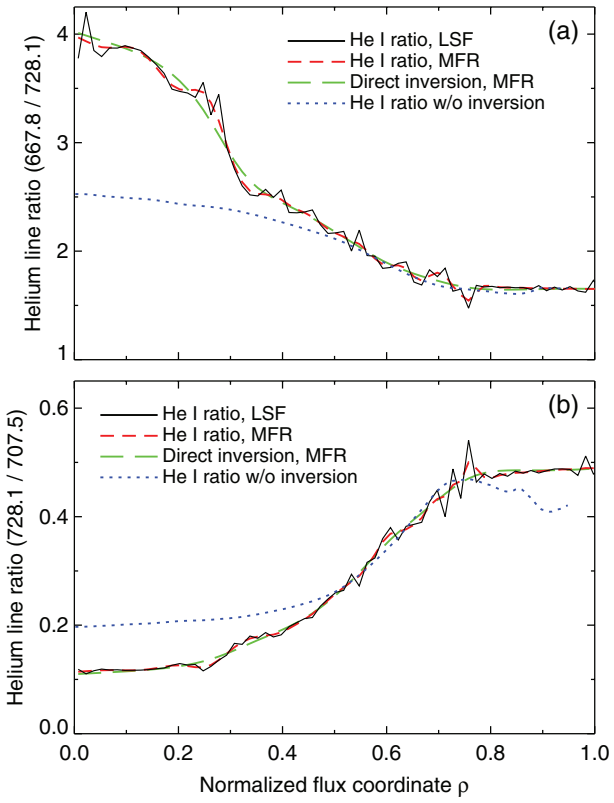

FIG. 7. Plasma radiance ratio profiles derived from the LSF and MFR reconstructions and from the direct inversion using Eq. (4), and the ratio profile derived from the line-integrated intensities without inversion: (a) He I 667.8/728.1 nm, for n_e measurements, and (b) He I 728.1/706.5 nm, for T_e measurements.

of the profiles in Fig. 5). The ratios near the edge of the plasma are in good agreement with the tomography reconstructed values. Towards the center of the plasma, the intensity ratio of the line-integrated measurements is much lower and higher than that from the tomography, respectively, for He I 667.8/728.1 nm and He I 728.1/706.5 nm. These differences are as expected because the line-integrated ratio close to the plasma center is approximately the average of the ratios along the line-of-sight path. The good consistency of the intensity ratios near the plasma edge indicates that the correction of the reflection at the edge of the plasma is reliable. The consistency also indicates that the line intensity ratio at these edge positions can be obtained without taking inversion for conditions in which the access to measurement of plasma emission from the total cross section is restricted. Therefore, the n_e and T_e at the edge of the plasma can be directly measured with a high-speed detector, which allows the possibility to extract plasma fluctuation information in this region.

Figure 8(a) shows the n_e profile inferred from the measured helium line radiance ratios based on the CR model calculations presented in Sec. II B and that from the tomographic reconstruction based on the interferometer measurements. The n_e determined by the line intensity ratio technique is the time averaged value within the camera exposure interval (see Fig. 2). The n_e profiles obtained from the interferometer are reconstructions at five different times within the camera exposure interval; the profiles shown in the plot represent the average, the upper and lower bonds of the measurements at the five time positions. The two diagnostic techniques yield very consistent n_e values at $\rho < 0.5$, whereas the n_e value from the line intensity ratio technique is somewhat higher than that from the interferometer at $\rho > 0.5$.

Figure 8(b) shows the T_e profiles obtained from the measured helium line intensities, He I 728.1 and He I 706.5 nm, with plasma n_e values obtained from He I 667.8/728.1 nm ratios and from the averaged interferometer measurements. For comparison we also show the inferred T_e profile for a plasma formed under comparable discharge conditions but using the ratio of atomic helium emission from a spatially localized supersonic injected gas beam at wavelengths 504.8 and 471.3 nm.[7,8] The results show hollow profiles for both plasmas and T_e close to the plasma center ($\rho < 0.4$) has an almost flat profile. This is the typical behavior of T_e for 0.5 T He/H discharges in the H-1 heliac where the bare RF heating antenna appears to deposit most of the injected energy in the outer region of the plasma. The T_e values for the two plasmas are in good agreement in the region $\rho < 0.6$. In the outer region, however, the T_e inferred from the He I 728.1/706.5 nm line ratio is about 20–30 eV higher than that in the case of the localized measurement.

For the measurement of n_e values using the helium line intensity ratio technique (He I 667.8/728.1 nm), it is important to notice that this method is only suitable for $n_e > 10^{12}$ cm^{-3} for which the results will have a relatively large accuracy. As shown in Fig. 1(a), for $n_e < 0.5 \times 10^{12}$ cm^{-3}, the He I 667.8/728.1 nm line ratio from the CR model for n_e measurements is not sensitive to n_e, while a strong function of T_e; a small variation in the line intensity ratios will cause a large difference in the inferred n_e values. Therefore, the

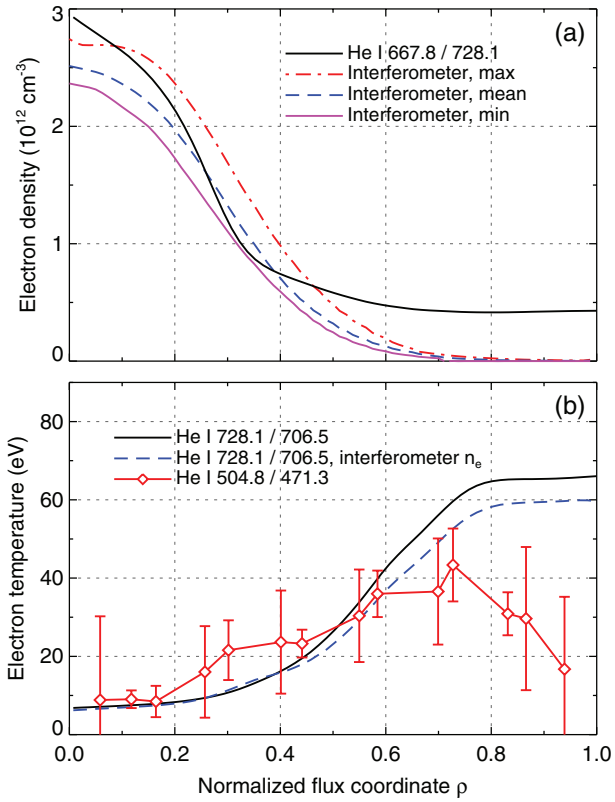

FIG. 8. (a) Plasma n_e distributions measured by helium line ratios, He I 667.8/728.1 nm, and by interferometer with vertical scans and inversion. (b) Plasma T_e distributions measured by tomography (this work) using helium lines, He I 728.1 and 706.5 nm, and using localized emission (He I 504.8/471.3 nm) from an injected supersonic beam.[7]

inconsistency of n_e values between the two diagnostic techniques at the edge of the plasma is possibly due to uncertainties in any or both of the measurement and the CR model. When considering the calibration errors, the n_e values at $\rho > 0.5$ are still too high. Since the helium line intensities measured at the edge of the plasma have a low signal-to-noise ratio and the determination of n_e is based on the ratio of the two spectral line intensities, minor uncertainties in the measurements such as due to reflection may cause large errors. Uncertainties in the CR model such as inaccuracy of atomic data and the radiation trapping may also lead to errors in the determined n_e values. The influence of radiation trapping on the measurements of n_e and T_e using the helium line intensity ratio technique have been extensively investigated.[21–23,27] It is shown that, by including the effects of radiation trapping in the CR model, the determined n_e and T_e values are in better agreement with probe measurements.[21–23] The theoretical line intensity ratio, He I 667.8/728.1 nm, for the n_e measurement increases when considering the radiation trapping using ray tracing simulation,[23] and thus the n_e values determined would be decreased in that case.

Notwithstanding the slightly different discharge conditions, there are some discrepancies between the measurements of T_e values using the different helium line intensity ratios. Because the He I 728.1/706.5 nm line ratio is a function of both T_e and n_e, an overestimate of the edge n_e values leads to a corresponding overestimate of T_e by about 7 eV (see the T_e profile obtained with n_e values from the interferometer in Fig. 8(b)). Second, the possible existence of hot electrons will cause an overestimate of T_e by at least 10 eV; the effect of hot electrons has been discussed in previous papers.[13,14] The low signal-to-noise ratio of the inverted edge radiances might also introduce errors that exaggerate the edge temperature. Finally, the uncertainties in the CR model should also be considered. The two helium metastable states (2^1S and 2^3S) in the CR model have been reported not to be accurately described by the steady state model.[16,17] If this is the case, we expect that the inferred T_e values with the CR model will be higher than those obtained with populations less dominated by the metastable states. Also, as in the case of the n_e measurements, the inclusion of radiation trapping will increase the theoretical line intensity ratios (He I 728.1/706.5 nm) for T_e measurements,[23] leading to a reduction in the inferred T_e values.

The helium CR model developed by Fujimoto[11] and Goto[12] has widely been used by many research groups for the determination of n_e and T_e using the line intensity ratio technique. After comparing with published works, we find that the updated CR model yields more accurate n_e measurements. Recently, Ohno *et al.*[24] have designed a two-dimensional optical system for simultaneously measuring n_e and T_e in the edge plasma of a small tokamak HYBTOK-II. The measured T_e values are in good agreement with those from probes, whereas the n_e values from the line ratio technique are about two times higher than probe measurements. If the n_e values are inferred from the updated CR model, the results will be in better agreement with the probe measurements. Therefore, the updated atomic data for the helium CR model cannot account for the higher n_e and T_e values at the edge of the H-1 plasma measured by the line intensity ratio technique.

V. CONCLUSIONS

Helium line intensity ratio technique based on a CR model has been used to infer n_e and T_e distributions in the H-1 heliac plasma. An inversion approach using minimum Fisher regularization has been used to directly reconstruct the line emission ratios from line-integrated intensity profiles. The n_e and T_e values determined by the line intensity ratio technique are reliable in the inner region of the H-1 plasma, while there remains some uncertainty at the edge of the plasma. Factors that may explain the discrepancy such as uncertainties in the measurements and physical processes neglected in the CR model have been considered and discussed. To resolve uncertainties in the measured n_e and T_e values at the edge of the plasma, further systematic measurements and comparisons with other diagnostics such as probes are required.

ACKNOWLEDGMENTS

The authors would like to thank John Wach and Horst Punzmann for continued support of the H-1 experimental operations. They also thank Mark Gwynneth for helping construct the optical measurement system and Michael Blacksell for designing the experimental control system. One of the

authors (S. Ma) thanks David Pretty for providing the plasma magnetic field data.

[1]N. Bretz, Rev. Sci. Instrum. **68**, 2927 (1997).
[2]S. M. Hamberger, B. D. Blackwell, L. E. Sharp, and D. B. Shenton, Fusion Technol. **17**, 123 (1990).
[3]J. Howard, C. Michael, F. Glass, and A. D. Cheetham, Rev. Sci. Instrum. **72**, 888 (2001).
[4]J. Howard and D. Oliver, Appl. Opt. **45**, 8613 (2006).
[5]S. T.A. Kumar, B. D. Blackwell, J. Howard, and J. H. Harris, Phys. Plasmas **17**, 082503 (2010).
[6]C. A. Michael and J. Howard, Rev. Sci. Instrum. **75**, 4180 (2004).
[7]S. M. Collis "The Development of a directional gas injection system for the H-1NF heliac" Ph.D. dissertation (Australian National University, 2007).
[8]S. M. Collis, R. Dall, J. Howard, D. Andruczyk, and B. W. James, J. Quant. Spectrosc. Radiat. Transf. **110**, 340 (2009).
[9]G. W.F. Drake and D. C. Morton, Astrophys. J., Suppl. Ser. **170**, 251 (2007).
[10]W. L. Wiese and J. R. Fuhr, J. Phys. Chem. Ref. Data **38**, 565 (2009).
[11]T. Fujimoto, J. Quant. Spectrosc. Radiat. Transf. **21**, 439 (1979).
[12]M. Goto, J. Quant. Spectrosc. Radiat. Transf. **76**, 331 (2003).
[13]S. Sasaki, S. Takamura, S. Watanabe, S. Masuzaki, T. Kato, and K. Kadota, Rev. Sci. Instrum. **67**, 3521 (1996).
[14]L. Carraro, G. De Pol, M. E. Puiatti, F. Sattin, P. Scarin, and M. Valisa, Plasma Phys. Controlled Fusion **42**, 1 (2000).
[15]R. F. Boivin, J. L. Kline, and E. E. Scime, Phys. Plasmas **8**, 5303 (2001).
[16]R. Prakash, P. Vasu, V. Kumar, R. Manchanda, M. B. Chowdhuri, and M. Goto, J. Appl. Phys. **97**, 043301 (2005).
[17]R. F. Boivin, S. D. Loch, C. P. Ballance, D. Branscomb, and M. S. Pindzola, Plasma Sources Sci. Technol. **16**, 470 (2007).
[18]T. Nakano, H. Kubo, and N. Asakura, J. Phys. B **43**, 144014 (2010).
[19]H. Kubo, M. Goto, H. Takenaga, A. Kumagai, T. Sugie, S. Sakurai, N. Asakura, S. Higashijima, and A. Sakasai, J. Plasma Fusion Res. **75**, 945 (1999).
[20]O. Schmitz, I. L. Beigman, L. A. Vainshtein, B. Schweer, M. Kantor, A. Pospieszczyk, Y. Xu, M. Krychowiak, M. Lehnen, U. Samm, B. Unterberg, and TEXTOR team, Plasma Phys. Controlled Fusion **50**, 115004 (2008).
[21]S. Kajita, N. Ohno, S. Takamura, and T. Nakano, Phys. Plasmas **13**, 013301 (2006); **16**(2), 029901 (2009) (erratum).
[22]D. Nishijima and E. M. Hollmann, Plasma Phys. Controlled Fusion **49**, 791 (2007).
[23]S. Kajita, D. Nishijima, E. M. Hollmann, and N. Ohno, Phys. Plasmas **16**, 063303 (2009).
[24]N. Ohno, K. Miyamoto, K. Kodama, S. Kajita, and K. Kitagawa, Contrib. Plasma Phys. **50**, 962 (2010).
[25]E. de la Cal, J. Guasp, and TJ-II Team, Plasma Phys. Controlled Fusion **53**, 085006 (2011).
[26]S. Ma, J. Howard, and N. Thapar, Phys. Plasmas **18**, 083301 (2011).
[27]Y. Iida, S. Kado, and S. Tanaka, Phys. Plasmas **17**, 123301 (2010).
[28]M. Anton, H. Weisen, M. J. Dutch, W. Linden, F. Buhlmann, R. Chavan, B. Marletaz, P. Marmillod, and P. Paris, Plasma Phys. Controlled Fusion **38**, 1849 (1996).
[29]W. H. Press, S. A. Teukolsky, W. T. Vetterling, and B. P. Flannery, *Numerical Recipes: The Art of Scientific Computing*, 3rd ed. (Cambridge University Press, Cambridge, England, 2007).